

JAAS

Accepted Manuscript



This is an *Accepted Manuscript*, which has been through the Royal Society of Chemistry peer review process and has been accepted for publication.

Accepted Manuscripts are published online shortly after acceptance, before technical editing, formatting and proof reading. Using this free service, authors can make their results available to the community, in citable form, before we publish the edited article. We will replace this *Accepted Manuscript* with the edited and formatted *Advance Article* as soon as it is available.

You can find more information about *Accepted Manuscripts* in the [Information for Authors](#).

Please note that technical editing may introduce minor changes to the text and/or graphics, which may alter content. The journal's standard [Terms & Conditions](#) and the [Ethical guidelines](#) still apply. In no event shall the Royal Society of Chemistry be held responsible for any errors or omissions in this *Accepted Manuscript* or any consequences arising from the use of any information it contains.

Morphology and characterization of Dematiaceous fungi on cellulose paper substrate using Synchrotron X-ray Microtomography, Scanning Electron Microscopy and Confocal Laser Scanning Microscopy in the context of cultural heritage.

H. M. Szczepanowska¹, D. Jha,² Th. G. Mathia³

¹ Museum Conservation Institute, Smithsonian Institution, Suitland MD, USA

² Nano-Science Center; Department of Chemistry; University of Copenhagen, Copenhagen, Denmark

³ C.N.R.S. Ecole Centrale de Lyon, Laboratoire de Tribologie et Dynamique des Systèmes, France (emeritus)

Key words: X-ray microtomography, synchrotron radiation, confocal laser scanning microscopy, biodeterioration of paper, Dematiaceous fungi

Abstract

Dematiaceous (black pigmented) fungi interact with the cellular paper matrix growing on the surface and in paper bulk. Fungi-induced stains are one form of such interaction and are referred to as biodeterioration when applied to cultural heritage material. The complexity of both, paper and living systems, such as fungi, requires multi-scale analysis. The surface topography and spatial distribution of fungal monilioid hyphae, branched and un-branched chains and morphology of isodiametric enlargements of spores and yeast-like cells on the surface of paper were imaged with correlative microscopy, combining the environmental scanning electron microscopy and imaging in backscattered electron mode (SEM-BSE) with confocal laser scanning microscopy (CLSM). The spherical fruiting bodies (perithecia) embedded in paper were not detected by CLSM, and ESEM provided data collected near the surface. Their interaction with paper was analyzed with 3D visualization with X-ray microtomography (X μ CT). Until now the fungi and paper interfaces in the matrix (bulk) of paper had not been analyzed with X μ CT. We present a novel method of investigating the interaction of fungal pigmented mycelium, spores and perithecia in the paper matrix using X μ CT and 3D visualization based on the X μ CT data. The tomographs were generated on the designated ID19 beam at ESRF, Grenoble, France. The ultimate purpose of this investigation was to understand the mechanisms of fungi and paper interactions in order to develop preservation strategies for cultural heritage, such as historic and artistic works on paper infested by fungi.

Introduction

Biodeterioration refers to an adverse action of fungi or bacteria manifested by staining and often the structural degradation of a material on which they grow. It is triggered by multitude of factors, the environment, the structure and composition of the materials and the nutritional preferences of microorganisms growing on them. Fungi induced pigmentation is difficult to reverse and once the material on which they grow is digested, the deterioration is irreversible. Therefore, understanding the mechanisms which govern different aspects of fungal life cycles is essential to both prevention of fungal infestation and, once it has occurred, its remediation or feasibility of any corrective action. This study is investigating one aspect of biodeterioration, namely, stains induced by Dematiaceous fungi on cellulose-based historic and artistic works, using correlative microscopy and X-ray microtomography.

Fungal pigmentation of paper results from complex interactions of heterogeneous cellular material (paper) with living systems (fungi). The fungal pigments, defined as secondary metabolites, are bi-products of

1
2
3 bio-chemical processes within fungal cells. The pigmented spores and mycelium of many colors produce
4 superficial stains on the surface of paper and inside the microstructure of paper referred to as matrix or
5 bulk. The structural degradation of paper fibers is caused by fungal enzymatic activities. This
6 investigation explores black stains on paper attributed to Dematiaceous, meristematic fungi and their
7 interactions with the paper matrix. These fungi represent a large group of organisms causing pathogenic
8 infections in plants and humans; over 100 species were isolated from humans [1]. They are ubiquitous
9 soil saprophytes. Those found on cultural heritage material were meristematic fungi that phylogenetically
10 belong to, or have association with, at least three different orders: *Chaetothyriales*, *Dothidiales* and
11 *Pleosporales*. [2] Their identification is difficult because of their ability to convert in various stages of
12 their life cycle from filamentous to yeast-like growth. Dematiaceous fungi do not possess any distinct
13 features, other than their common black pigmentation, attributed to melanin in their cell walls. Because
14 they grow in demanding environments of extreme temperatures, with scarcity of nutrient and limited
15 availability of water, UV radiation and oxygenic action, they are very resilient to any potential
16 remediation actions. That, and the difficulty in characterizing their morphology are most likely the
17 reasons why Dematiaceous fungi received very little attention in the context of cultural heritage. These
18 fungi were reported growing on rocks, marbles and granite in extreme temperatures, from the desert of
19 Arizona to the cold of Antarctic, in environments with limited nutrients and water availability [3,4]; only
20 two references noted their presence on paper [5,6].
21
22
23

24 Optical microscopy provided information about meristematic fungi growth patterns which led to the
25 formation of stains. Environmental scanning electron microscopy in variable pressure (ESEM),
26 traditionally utilized for the investigation of paper and biological specimens, revealed topography of
27 paper surface and morphology of fungi features, both imaged in backscattered electron (BSE) mode. The
28 spatial distribution of fungal spores and mycelium on the paper surface was obtained with confocal laser
29 scanning microscopy (CLSM). The results produced by correlative microscopy, where the same sample is
30 analyzed using two or more techniques differing in scales (macro- to micro-), permitted interpretation of
31 data generated by X-ray microtomography (X μ CT). The 3D visualization based on X μ CT data shows the
32 growth patterns of fungi in the paper internal structure complementing the results obtained in ESEM and
33 CLSM. Although X-ray microtomography has been successfully utilized before to characterize features of
34 paper fibers, pores and additives to paper [7,8] to the authors' knowledge this technique has only now
35 been applied for the first time to the investigation of microorganisms growing on paper [9]. The
36 experimental setting of X μ CT and data processing aiming to produce the 3D visualization are discussed.
37 The findings contribute to the design of preservation strategies applied to cultural heritage and elucidating
38 difficulties of removing bio-deposits from paper.
39
40
41

42 **Materials and methods**

43 **2.1 Samples**

44 Two historic papers affected by black fungal stains were used in this study; (1) a 17th century handmade
45 sheet from the collection of the Maltese Archives in Malta, and (2) a 1920 Engraving on machine-made
46 paper. The total number of stains analyzed was 26 and 14 on each paper respectively. The fiber
47 composition of both papers was cotton, as determined based on the fibers' morphology.
48
49
50

51 Two types of stains caused by different fungi species were analyzed on the 17th century paper, sheet size
52 233mm x 170mm. One type (1A) was produced by the congregation of pigmented spores, and the other
53 (1B) by large dark brown to black fruiting bodies, perithecia, 50-100 μ m embedded in paper. The stains'
54 diameter in (1A) was 0.5mm-2mm (fig.1).
55
56
57
58
59
60

The 1920 Engraving on paper, sheet size 352mm x275mm, showed black fungal stains along the top edge of the sheet; the stains' diameter was similar to the 1A type, 1mm-2.6 mm. The pigmented fungal mycelium and spores' chains, however, expanded outside the stains' perimeter reaching up to 4.5 mm span (fig.2).

The samples of stained papers, 1mm x 1mm, were extracted from the 17th century paper (1A and 1B type) and from the 1920 Engraving. All samples were conditioned for 6hrs in a controlled environment, RH 46.6% and T 22.3°C, prior to X-ray microtomography radiation. No preparation of samples was necessary for SEM-VP. The CLSM imaging was carried out in situ, in room temperature 22°C, without extracting samples from the original papers.

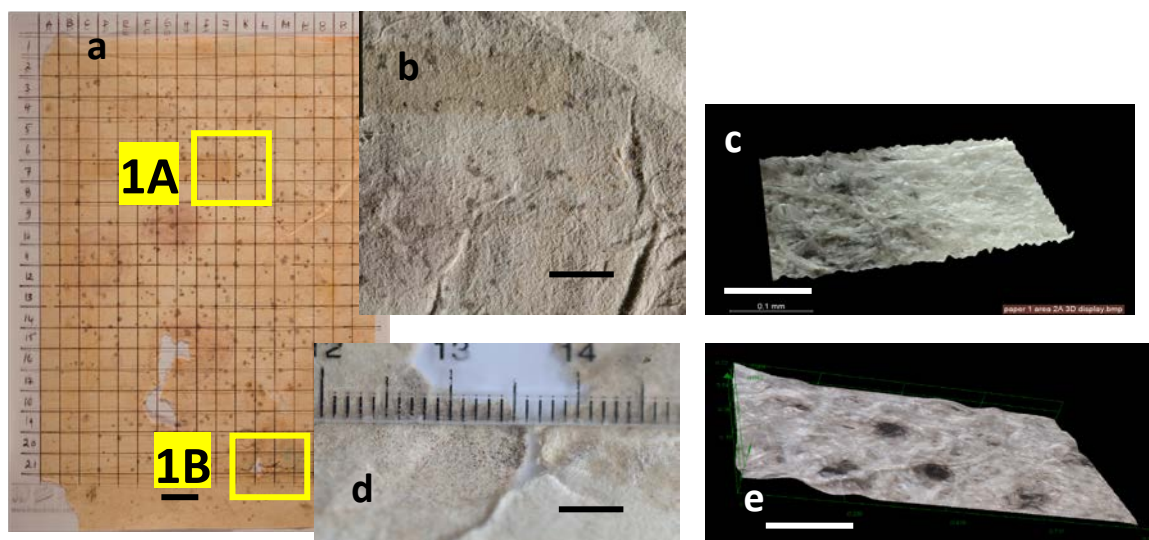


Fig.1.a The 17th century paper with fungal stains, (1A) formed by clusters of cells and (1B) by large fruiting bodies. The areas of analysis are marked with yellow squares; scale bar 20mm. 1.b) Type (1A) stains, scattered on paper, are made of pigmented clusters of spores. Optical micrograph, scale bar 20mm. 1.c) A view of (1A), in extended depth of field shows fungal spores on the surface, concentrated in indentations among paper fibers; scale bar 0.1mm. 1.d) Stain type (1B), inclusions of dark, large fruiting bodies (perithecia), scale bar 5mm. 1. e) A composite micrograph of (1B) in extended depth of field shows individual dark, fruiting structures; scale bar 0.1mm

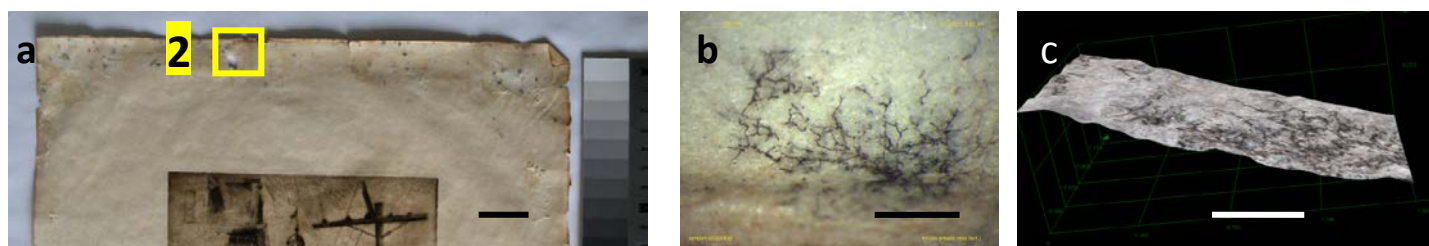


Fig.2 a) The 1920 Engraving shows black fungal stains along the top edge; scale bar 20mm. 2. b) A micrograph of the stain shows the pattern of fungal growth as black trailing filaments; scale bar 0.5mm.

1
2
3 2.c) A composite micrograph in extended depth of field shows fungal deposits on the surface of paper;
4 scale bar 0.1mm.
5
6

7 **2.2 Analytical methods**

8
9 The environmental (or, variable pressure VP) scanning electron microscope (ESEM), 3700 N Hitachi,
10 with low vacuum was used for analysis of paper topography and morphology of fungal deposits on the
11 surface of paper. The micrographs were taken in backscattered electron mode (BSE). The analysis and
12 imaging were carried out under following conditions: 15-40Pa, 12-15kV, magnification range 300x-
13 3000x. ESEM is one of the imaging surface analysis techniques which we utilized to obtain information
14 about surface topography of both paper and fungal deposits and spatial distribution of fungi.
15
16

17 The Confocal Laser Scanning Microscope (CLSM), VK 9700, with a violet light source (408 nm) and
18 photomultiplier detector to increase light intensity combined lateral scanning (x, y direction) with a
19 confocal laser probe. The height, z direction, was 'sensed' based on the depth of focus of the objective.
20 Although CLSM can focus and scan sections of a sample in z-plane, resulting in high resolution 3D
21 surface imaging, the depth of CLSM is limited. The advantage of CLSM is based on eliminating light
22 from points other than analyzed, focal point, thus increasing the amount of light received in 'z' direction
23 which collects the height data. The optical image is captured by CCD image sensor. The high resolution
24 surface images obtained from ESEM supplement this analysis serving as a verification standard for
25 images obtained at the top sections of an analyzed sample. Only one type of laser source can be used at a
26 given time, which limits the application of CLSM and requires thoughtful selection of the laser from the
27 onset. (Further analysis of multi-scale characterization of fungal deposits see: Szczepanowska, Mathia,
28 Belin, *Scanning*, 2012 [5]).
29
30

31 The X-ray microtomography was carried out at the European Synchrotron Radiation Facility (ESRF)
32 Grenoble, France on ID19, X-ray imaging and diffraction beamline. It is a long beam, 145m, dedicated to
33 X-ray tomography and topography [10]. The samples were set on a vertical rotating stage (fig.3) and the
34 CCD-high resolution X-ray image detector captured projected images, generated by the passing beam.
35 Each sample in our experiment was rotated 360 degree around the vertical axis, perpendicular to the X-
36 ray beam, with 1500 angular steps. At each step a radiograph was collected. Thus obtained radiographs
37 were used to reconstruct the 3D digital image of the sample. Conditions of the experiment were as
38 follows: 30 keV, time of data acquisition 0.5 -2s, voxel size $0.7 \mu\text{m}^3$ and paper samples size, 1mm x 1mm
39 x paper thickness. The field of view was $1400\mu\text{m} \times 1400\mu\text{m} \times$ paper thickness, which was averaged as
40 $500\text{-}800 \mu\text{m}$, based on its similarity to Whatman paper [11]. The thickness of paper was uneven due to
41 random distribution of fibers in this hand-made sheet, deposits in paper and in some areas partial
42 digestion by fungi. 3D structure of paper is orthotropic. The beam size at the sample position, with
43 (maximum) dimensions $45 \times 15 \text{ mm}$ depending on the energy level at a given time.
44
45
46
47

48 The 1mm x 1mm paper samples were attached with self—adhesive tape to a glass capillary which in turn
49 was secured onto the rotating stage with microcrystalline wax. The mounting method for paper samples
50 was developed by J-F Bloch and his research group at the Laboratory of Pulp and Paper Science and
51 Graphic Arts, Grenoble, France.
52
53
54
55
56
57
58
59
60

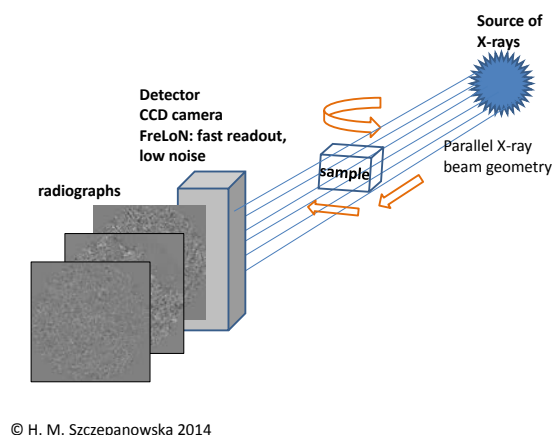


Fig. 3 A schematic, not to scale, diagram of the X-ray tomography experimental set up. The synchrotron source produces parallel X-ray beam so the sample is not magnified on the detector CCD, FreLoN camera. The parallel, monochromatic beam set-up ensures accurate quantitative reconstruction of the microstructure.

2.3 3D visualization and X-ray tomography data processing

The tomograms of the samples were generated at ID19 beamline at ESRF by the beam that falls on a sample in parallel configuration. The low noise CCD detector gives projections of size 2048^2 pixels that are used to reconstruct a 3D volume of 2048^3 voxels by PYHST software [12]. The voxel size of the 3D data was $0.7\mu\text{m}^3$. The setup details for ID19 tomography can be found elsewhere [13,14]. Fungi and paper fibers are resolved in the tomograms for stain (1A) in fig. 4e and for stain (1B) in fig 5c,d. The X-ray attenuation coefficient for both paper and fungi were in same orders of magnitude, that means they absorb the X-rays equally, producing images with no contrast difference. This complicated the segmentation process, which was crucial for quantitative analysis. To enhance the possibility of reliable segmentation, we started by suppressing the ring artifacts which come from inhomogeneity in the response function of detector elements [15] wavelet filtering the noise [16]. Additional challenge lied in similarities of paper fibers and fungal mycelium. The fungal spores on the other hand were small and ellipsoidal. Although the size of some compacted fungal fruiting structures, like perithecia in stain (1B), were in nearly the same order of magnitude as the paper fibers. However, the texture, shape and size of fungi spores differ from paper which allowed their separation for further analysis.

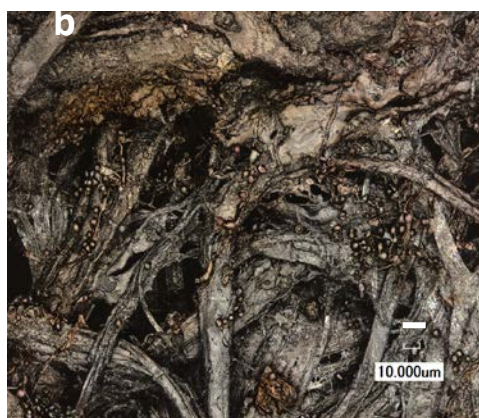
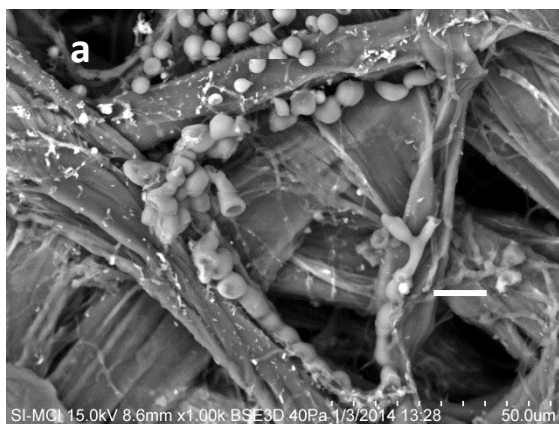
We exploited these differences, size and the sphericity of fungi to segment the spores from the paper fibers. The fungi and paper fibers in the sample 1B, with perithecia, dark compacted fruiting bodies ($50\text{-}100\mu\text{m}$), we classified deploying WEKA tool available for ImageJ software [17]. Thus separated phases were then segmented out based on their size and sphericity [18]. More complex process was employed in visualization of stains formed by clusters of spores which revealed presence of small ($3\text{-}6\mu\text{m}$) and larger particles ($4\text{-}16\mu\text{m}$).

For the stain (1A) the following operations were carried out:

1. The features on each tomogram slice were enhanced by adding each slice with its variance image multiple times keeping the variance parameter $\sigma^2 = 5$, thus selecting the features greater than 5 pixels.
2. Segmentation used Otsu method which is described in [19]. This method minimizes the variances between two classes present in the tomography image. Here, the objects (paper and fungi) were separated from their background. This was necessary to ensure that later operations would exclude unnecessary pixels.
3. 3D watershed transformation was used to separate the overlapping spores. Some spores, especially in colonies, were positioned so close to each other that the X μ -T could not resolve them as separate particles; they looked like one big cluster. This operation aimed to separate such, almost connected, spores to ensure fair analysis of individual spores.
4. The objects were classified in the 3D data based on sphericity and size and a binary mask was created.
5. The 3D mask from step 4 was multiplied with original 3D data to obtain spores-only volume.
6. The volume obtained in step 5 was subtracted from the original image to obtain paper fiber-only volume.

In sample (1B) about 74 % of the paper volume was occupied by paper fibres and fungi and the remaining 24% were voids. In the sample (1A) the paper fibres and fungi occupied only 50% which can be explained by smaller size of fungal cells in comparison with large perithecia in (1B). The geometric properties of the segmented fungi were obtained by calculating the ellipsoidal fit on the segmented fungi, as seen in fig.5d. It shows the ellipsoid fit on the compacted fungi fruiting body, which is concealed within the paper fibers. The fungal aggregate in stains formed by dark compacted fungi (1B) were found to be buried 50 μm into the paper (2·a), and had the lateral spread of 87 μm in one direction (2·b) and 109 μm in the other (2·c) as shown in fig. 5d. By contrast to that compact structure, fig. 4e shows the fungal spores scattered on the surface of paper fibers in stains (1A) type.

In total, 12268 spores were identified in the sample (1A), with an average spore volume of 7-20 μm^3 , as seen on the bargraph in fig.4.f. The processing as described was carried out in MATLAB and ImageJ [17]. The 3D visualization was prepared in imageJ and Avizo fire.



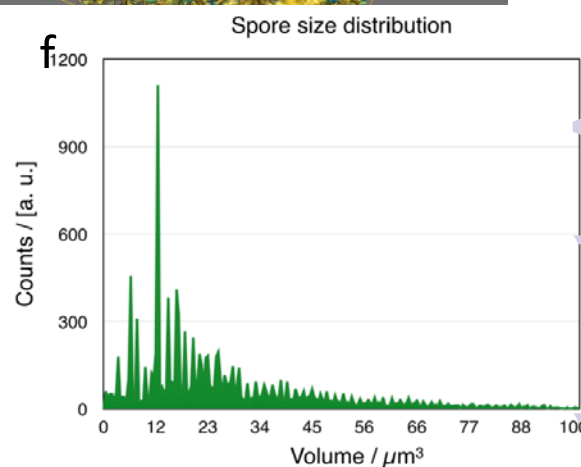
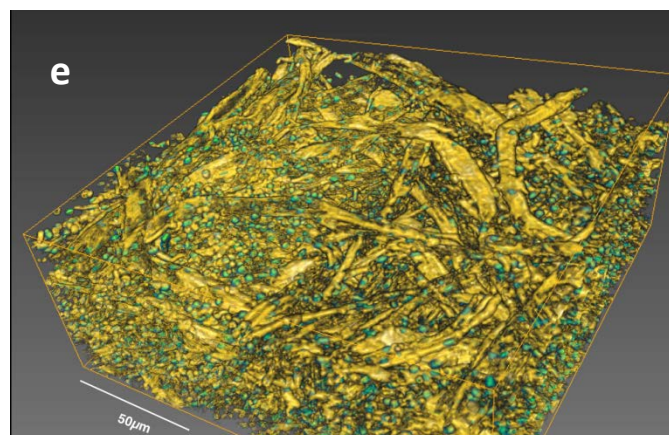
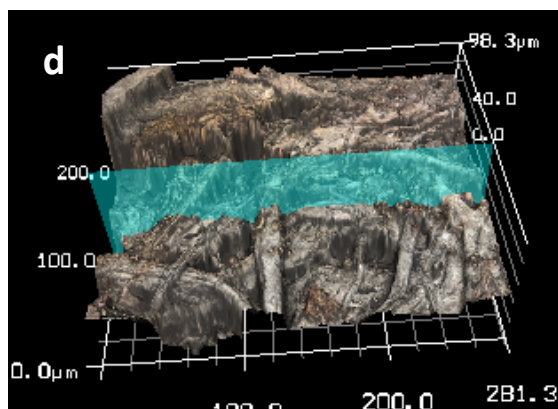
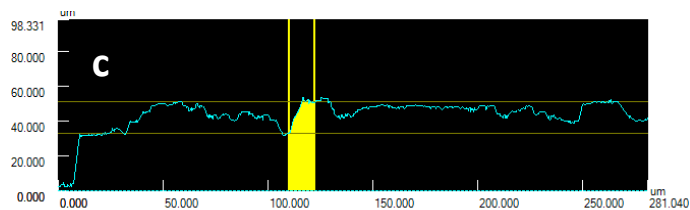
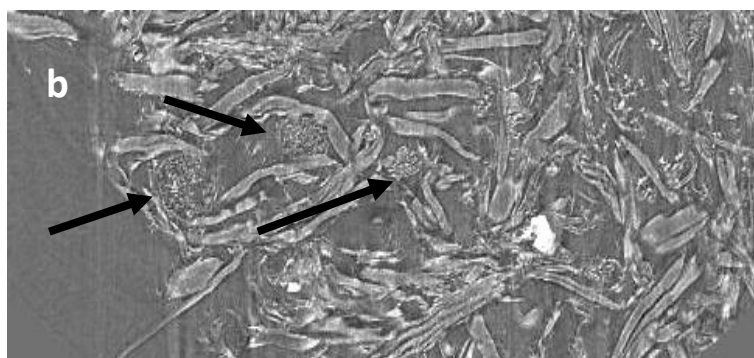
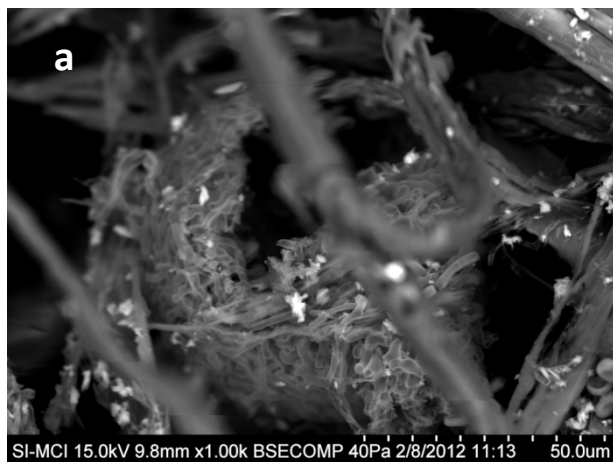


Fig.4. a) Fungal stains on paper (1A) analyzed in multi-scale regime. ESEM, spores 3-6 μ m show thigmotropism, cells following texture of the paper fibers' surface. Branching mycelium is visible in the 5o'clock position; scale bar 10 μ m. 4. b) CLSM, spatial distribution of fungal spores, small spherical deposits on the surface of paper fibers; scale bar 10 μ m. 4.c) CLSM path of scanning across the surface with fungal deposits, 282 μ m long scan path. 4.d) Profile obtained with two-line CLSM scan shows increase in height of 39,1 μ m attributed to both paper topography and spores on the surface of paper. 4.e) 3D visualization obtained based on X μ CT data. Green particles are individual spores on the surface of paper fibers. 4.f) Using spores' size as a criteria, distribution of spores was analyzed in the entire volume of 22941356 μ m³ most of them were 7-20 μ m.



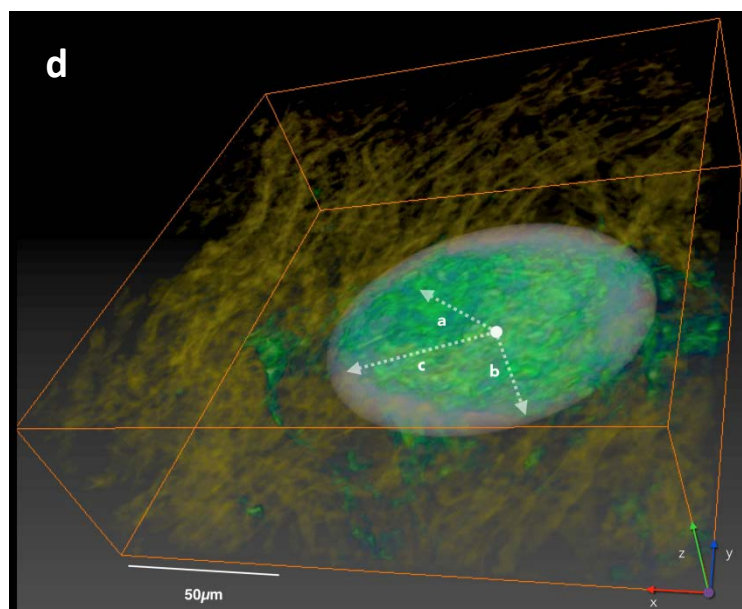
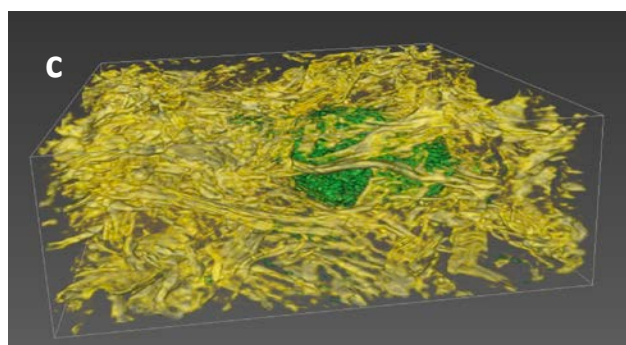


Fig. 5 Stain (1B), formed by a large spherical fungal fruiting structure (perithecium) 60-100 μm. 5.a) ESEM micrograph, top view of partially damaged perithecial wall; scale bar 10 μm. 5. b) 3D cross-section of X-ray tomography with arrows points to perithecia embedded in the paper matrix. 5.c) 3D visualization shows green inclusions in the paper matrix. 5.d) The ellipsoid fit on the compacted fungi fruiting body, which is concealed within the paper fibers, shows directionality of measurements.

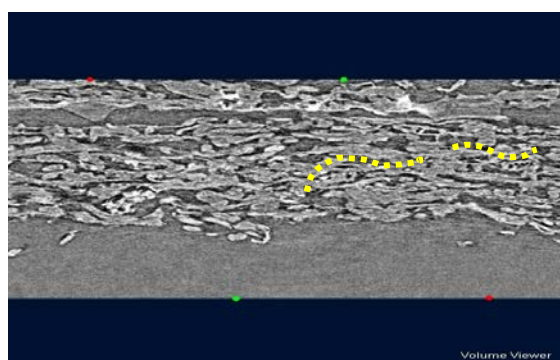
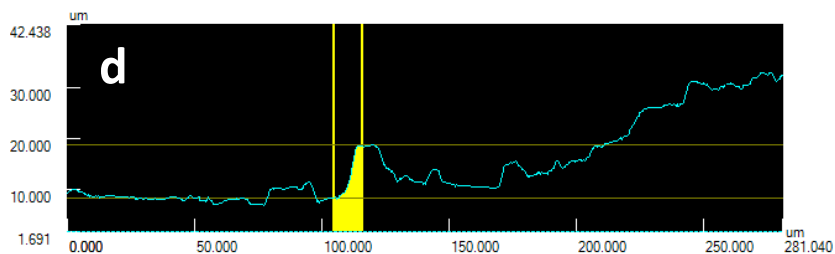
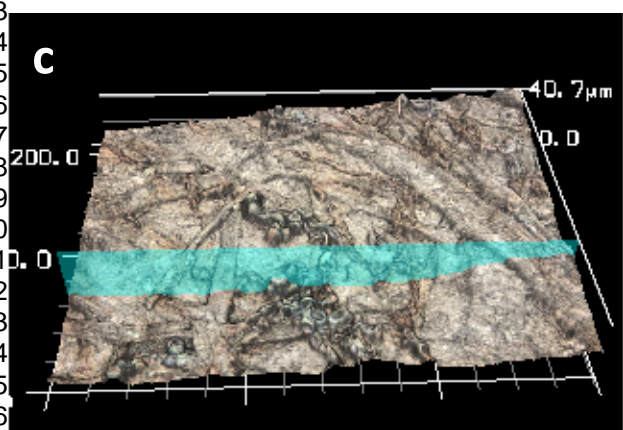
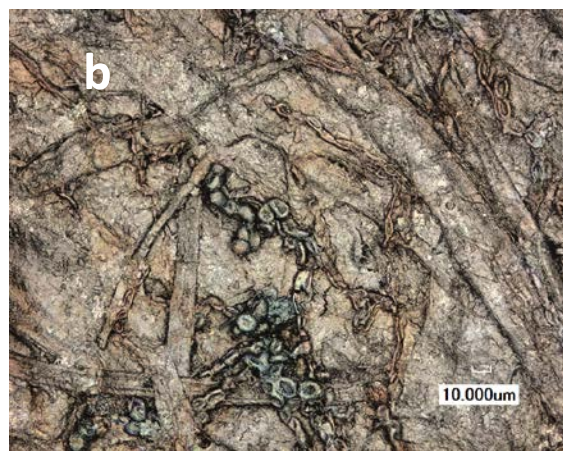
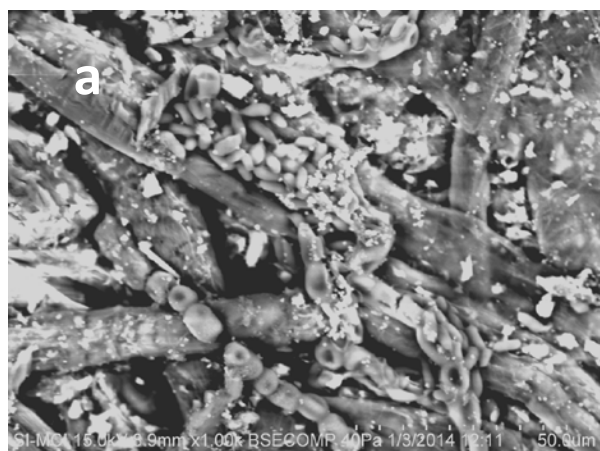


Fig.6.a) Stain on paper (2), ESEM micrograph shows robust spores in catenulate (in rows and chain-like) formations, cells' dimensions 5-9 μ m, and another type, uniform and elongated 4-6 μ m.6. b) CLSM micrograph of spatial distribution of fungal spores shows two distinct shapes of spores, larger spherical deposits and chainlike; scale bar 10 μ m. 6. c) CLSM path of scanning across the surface, 281 μ m distance. 6.d) Profile obtained with two-line CLSM scan shows increase in height of 23.2 μ m attributed to both paper topography and spores on the surface of paper. 6.e) X μ CT tomograph, a cross-section showing a compact paper and fungal inclusions as chains among fibers, marked with yellow lines.

Results and discussion

The application of multi-scale analysis revealed different morphological features of fungal deposits and their interfaces with paper matrix and paper fibers' surface. A statistical computation of fungal particles in (1A) derived from X μ CT data indicated large number of yeast-like cells (7-20 μ m) in addition to smaller fungal spores (3-6 μ m). That finding of two distinct groups of spores varied in size was possible through the 3D visualization. The ESEM images showed topography of the paper fibers and fungal deposits. The paper fibers of both (1) and (2) are well preserved, indicating handmade sheet (1) and carefully processed machine paper (2). The topography of the paper surface in the 17th c. sheet indicated loose arrangement of fibers, while the 1920 Engraving showed a more compact paper matrix. Both configurations of the paper matrix impacted fungal growth.

Investigation of biological samples with synchrotron radiation is particularly challenging because these specimens produce little contrast in x-ray images. (In a sample from the 1920 Engraving, 3D visualization was unattainable due to poor contrast). One of the methods of visualizing structures with poor absorption contrast is to 'stain' the samples with metal compounds which have high X ray attenuation coefficient. This is analogous to a fluorescence label applied to biological samples in light microscopy. The metal elements that have been reported for contrasting biological microstructures include gold, platinum and silver [20]. That is one area which we are planning to explore in our future studies.

Another method which we consider in our future work is holotomography [21]. Beamline ID 22 which is enhanced and renamed ID19 at ESRF, currently produces the tomograms of voxel resolution down to 25 nm [22] and lower. The reduction of voxel resolution means that the size of the voxel is going to increase therefore this argument relies on inverse proportionality. The quantitative analysis of the distribution of phases present in the sample can be more accurately defined with such very high resolution tomography techniques. This two-prong approach ('staining' and very high resolution tomography) should result in obtaining highly detailed 3D distribution and growth patterns of fungi in the paper matrix. Furthermore, we will explore statistical analysis of fungi distribution, size of fungal propagulates and relationship of their deposits to volume of fibers and voids in paper. The wealth of data obtained via X-ray microtomography opened a broad range of potential for analysis and interpretation.

The CLSM showed that spatial distribution of fungal spores on the surface conformed to the papers' topography by clustering in indentations, congregating along paper fibers and burrowing into paper matrix. The spatial distribution of fungi on the surface of papers and variations in spores' shape was clearly imaged with CLSM, showing their intricate interaction with paper fibers, which most likely provided physical anchorage for fungal mycelium. The spores appeared to be attached to the surface of paper fibers in both cases (1A) and (2) and utilized indentations in the paper surface most likely as a protection mechanism against their removal by mechanical forces, air movement or brushing off. The observed differences in fungal spores showed cells that are semispherical and oval, different in size, 3-6 μ m and 4-16 μ m in paper (1A) and robust, thick-walled and larger, 6-9 μ m, on paper (2). The catenulate cells in (1A) showed thigmotropism, cells following texture of the paper fibers' surface (fig.2a,b, 4a,b). That was confirmed on ESEM micrographs of fungi on both papers that showed morphology of thick-walled spores in aggregates, as clusters, and in catenulate formations, along the paper fibers in (1A) and (2). That, combined with morphology of isodiametric enlargements of spores and yeast-like budding cells,

1
2
3 especially in stains (1A) and (2) and X μ CT statistical analysis of cells' size pointed out to Dematiaceous,
4 meristematic fungi. The ESEM analysis also indicated monilioid hyphae, branched and un-branched
5 chains in (1A) and (2). The ESEM images of (1B) stain caused by large pigmented fruiting structure,
6 showed only its top view, indicating that the remaining part was embedded in the paper matrix. X μ CT
7 revealed the depth of this inclusion, thus its shape and complete set of dimensions.
8
9

10 The interactions inside the paper matrix were visualized based on X μ CT data and provided information
11 about the interactions of fungal mycelium, spores and fruiting bodies inside the paper matrix.
12 Furthermore, this analysis indicated the three-dimensional characteristics of fungal deposit, dimensions
13 and depth of their penetration into paper. Large fruiting structures were embedded in paper matrix rather
14 than formed on the surface, following survival mechanisms of microorganisms, protecting themselves
15 against environmental factors, such as excessive exposure to light. X μ CT complemented the information
16 from data obtained in CLSM and ESEM. The 3D visualization revealed that in all cases fungi became an
17 integral part of the paper's microstructure which would make their removal nearly impossible without
18 disturbing the paper matrix itself.
19

20 21 22 **Conclusion**

23
24 The data obtained in each analysis complemented each other and enabled a meaningful interpretation of
25 findings. The interpretation of data generated by X-ray microtomography aiming to detect fungi in the
26 paper matrix and determine their interfaces requires knowledge of both fungal morphology and
27 characteristics of paper. That is especially important in differentiation between morphology of fungal
28 mycelium, often tubular and elongated in shape, and fibrous paper matrix. The size of fungal spores
29 present, their shape, mostly spherical to oval, guided our ability to distinguish them in a fibrous paper
30 matrix. X μ CT revealed much larger number of yeast cells, size 7-20 μ m, which was not indicated by any
31 other analysis. X μ CT also provided information about depth of perithecia inclusion which was not
32 possible with the other two techniques (ESEM and CLSM). X-ray tomography is a powerful tool in
33 characterization of microstructures which are not accessible with the traditional analytical tools and
34 methods. It might become a valuable technique in characterizing biodegradation and defining the
35 relationship between fungal growth and the paper substrate as a complementary technique to ESEM and
36 CLSM. Although application of 3D visualization has been utilized in many fields, for example in
37 semiconductors, biological tissue [23], paper characterization [24] (Ramaswamy et al 2001) and
38 crystallography, its application in biodeteriorated cultural material until now has not been reported.
39
40

41
42 The 3D visualization permitted us better understanding of the intricate interactions between the paper
43 matrix and fungal mycelium and spores, elucidating the enormous challenge of physical removal of the
44 pigmented fungi. Numerous attempts have been made over the years to remove these disfiguring fungal
45 deposits from paper. However, the results are only partially successful. The underlying reason is an
46 intricate spatial distribution of fungal deposits in the paper matrix, as it was revealed by the X-ray
47 microtomography. The stain-forming pigmented spores are not only deposited on the top surface of the
48 paper fibers, but throughout the entire bulk. The implication of that finding points to devising remediation
49 methods that would rely on target-focused removal techniques. Laser cleaning, reported earlier by one of
50 the authors[25] was successful in evaporating the top -surface deposits. Most recent advances in nano-
51 technology, in particular nano-particles depositions, at times effective in retardation of fungal growth in
52 the textile industry, and nano-robotic devices, are some of the potential methods that should be
53 considered for further exploration.
54
55
56
57
58
59
60

Acknowledgements

The authors are indebted to S. Rolland du Roscoat and J.-F. Bloch, Ecole Française de Papeterie et des Industries Graphiques, for facilitating access to ESRF. We thank Scott Whittaker, SEM Lab Manager for his assistance with images in the extended depth of field.

References:

- [1] P.G. Pappas, Dematiaceous fungal infections. In, Goldman's Cecil Medicine, Lee Goldman and Andrew I. Schafer, 24th edition, Elsevier, 2012.
- [2] K. Sterflinger, G.S. de Hoog, and G. Haase. Phylogeny and ecology of meristematic Ascomycetes. *Studies in Mycology*, 1999, **43**:5-22.
- [3] K. Sterflinger and W. E. Krumbein, Dematiaceous fungi as a major agent for biopitting on Mediterranean marbles and limestones. *Geomicrobiological Journal*, 1997, **14**:219-230.
- [4] C. Urzi et al. Biodiversity of the rock inhabiting microflora with special reference to black fungi and black yeasts. In *Microbial Diversity and Ecosystem Function*, eds. Allsopp, D. Colwell, R. R. and D. L. Hawksworth, 1995: 289-302.
- [5] H. M. Szczepanowska, Th. Mathia and P. Belin, Morphology of fungal stains on paper characterized with multi-scale and multi-sensory surface metrology. *Scanning*, 2013, **36**:76-85.
- [6] H.M. Szczepanowska and Y. Goreva, "SEM and ToF-SIMS Ion Imaging Applied to Characterization of Fungal Biodeterioration of Paper in the Context of Cultural Heritage Collections". *Microscopy and Microanalysis*, 2014, Conference Preprints, M&M 2014, Hartford, CT.
- [7] P Vernhes, S. Rolland du Roscoat, A Blayo, B Pineaux, X thibault and J-F Bloch, Synchrotron X-ray Microtomography: A new tool to characterize the interactions between paper and toner. *JIST*, 2008, **52**(1):010502-6.
- [8] J-F Bloch, S Rolland du Roscoat, C. Mercier, P Vernhes, B Pineaux, A Blayo, and M Mangin, Influence of paper structure on printability: characterization using X-ray synchrotron microtomography. *Proc IS&T*, 2006 :449-453.
- [9] H. M. Szczepanowska, Living systems on heterogeneous cellular substrate: contribution to a better understanding of dynamic interfaces of fungal pigmentation and paper in biodeterioration of cultural heritage. Doctoral Dissertation, LTDS, University of Lyon, France, 2012.
- [10] http://www.esrf.fr/exp_facilities/ID19/homepage/id19homepage.html
- [11] https://us.vwr.com/store/catalog/product.jsp?product_id=4635485
- [12] A. Mirone, E. Brun, E. Gouillart, P. Tafforeau, and J. Kieffer, Nuclear Instruments and Methods in Physics Research Section B: *Beam Interactions with Materials and Atoms*, 2014, **324**: 41-48. <http://dx.doi.org/10.1016/j.nimb.2013.09.030>
- [13] L.Helfen, T. Baumbach, P. Cloetens, and J.Baruchel, *Applied Physics Letters*, 2009, **94**, 104103, DOI:<http://dx.doi.org/10.1063/1.3089237>.
- [14]: P. Cloetens¹, W. Ludwig¹, J. Baruchel¹, D. Van Dyck², J. Van Landuyt², J. P. Guigay³ and M. Schlenker³, Holotomography: Quantitative phase tomography with micrometer resolution using hard synchrotron radiation x rays, *Applied Physics Letters*, 1999, **75**, 2912-2914, DOI <http://dx.doi.org/10.1063/1.125225>
- [15] D. Jha, H. O. Sørensen, S. Dobberschütz, I. R. Feidenhans'l, and S.L.S. Stipp, Adaptive center determination for effective suppression of ring artifacts in tomography images, *Applied Physics Letters*, 2014, **105**, 143107 DOI: <http://dx.doi.org/10.1063/1.4897441>
- [16] F. Luisier, The SURE-LET Approach to Image Denoising, 2010, Swiss Federal Institute of Technology Lausanne, EPFL Thesis no. 4566.

- 1
2
3 [17] C. A. Schneider, W.S. Rasband, and K.W. Eliceiri, NIH Image to ImageJ: 25 years of image analysis,
4 *Nature Methods*, 2012, **9**: 671–675,. <http://doi:10.1038/nmeth.2089>
5 [18] H. Wadell, Volume, Shape and Roundness of Quartz Particles, 1935, *Journal of Geology* **43** (3):
6 250–280. doi:10.1086/624298.
7 [19] N. Otsu, A threshold selection method from gray-level histograms. In, Transactions on Systems,
8 Man and Cybernetics, *IEEE*,1979, **9**, (1): 62-66.
9 doi: <http://10.1109/TSMC.1979.4310076>
10 [20] R. Mizutani, A. Takeuchi, K. Uesugi, S. Takekoshi, R.Y. Osamura, and Y. Suzuki, 2010, Unveiling
11 3D Biological Structures by X-ray Microtomography. *Microscopy: Science, Technology, Applications*
12 *and Education*. A. Méndez-Vilas and J. Díaz (Eds):379-386. [http://www.formatex.info/microscopy4/379-](http://www.formatex.info/microscopy4/379-386.pdf)
13 [386.pdf](http://www.formatex.info/microscopy4/379-386.pdf)
14 [21] P. Cloetens, W. Ludwig, J. Baruchel, D. Van Dyck, J. Van Landuyt, J.P. Guigay, M. Schlenker,
15 1999, Holotomography: quantitative phase tomography with micrometer resolution using hard
16 synchrotron radiation x-rays. *Appl. Phys. Lett.*, **75**: 2912-2914.
17 [22] J. Villanova, J. Laurencin, P. Cloetens, P. Bleuet, G. Delette, H. Suhonen, and F. Usseglio-Viretta,
18 2013, 3D phase mapping of solid oxide fuel cell YSZ/Ni cermet at the nanoscale by holographic X-ray
19 nanotomography, *Journal of Power Sources*, **243**: 841-849, ISSN 0378-7753.
20 <http://dx.doi.org/10.1016/j.jpowsour.2013.06.069>.
21 [23] Baruchel J. Buffière J. Maire E. Merle P. and Peix G (eds), 2000, *X-Ray tomography in material*
22 *science*, Hermes, Paris.
23 [24] S. Ramaswamy, S. Huang, A. Goel, A. Cooper, D. Choi, A. Bandyopadhyay, and B.V. Ramarao,
24 2001, The 3D structure of paper and its relationship to moisture transport in liquid and vapour forms. The
25 science of paper making, 12th Fundamental Research Symposium, Oxford, UK, **2**:1289–1311.
26 [25] H. Szczepanowska, W. Moomaw, Laser Stain Removal of Fungus Induced Stains from Paper, 1994,
27 *Journal of the American Institute for Conservation (JAIC)* **33** (1):25-32; ISSN 0197-1360.
28
29
30
31
32
33
34
35
36
37
38
39
40
41
42
43
44
45
46
47
48
49
50
51
52
53
54
55
56
57
58
59
60